

Laser Induced Formation of Buried Void Layer in Silicon

T. Sameshima^{*1}, Y. Kanda ^{*1}, M. Hasumi^{*1}, J. Tatemichi^{*2}, Y. Inouchi^{*2}, and M. Naito^{*2}

^{*1}Tokyo University of Agriculture and Technology, 2-24-16, Naka-cho, Koganei, Tokyo, 184-8588, Japan

Email: tsamesim@cc.tuat.ac.jp

^{*2}Nissin Ion Equipment Co.,Ltd. Koka, Shiga 528-0068, Japan

Buried void layer formation in silicon substrates was achieved by hydrogen ion implantation followed by 940-nm infrared laser rapid heating. P-type silicon substrates coated with 100-nm-thick thermally grown SiO₂ layers were implanted with hydrogen atoms at 5×10^{15} and $3 \times 10^{16} \text{ cm}^{-2}$ at 60 keV. Structural investigation with analysis of optical reflectivity spectra revealed that $3 \times 10^{16} \text{ cm}^{-2}$ implantation caused a void layer with a void ratio of 0.04 at a depth of 250 nm close to the position of hydrogen peak concentration. Laser irradiation at $4.2 \times 10^4 \text{ W/cm}^2$ increased the void ratio to 0.12. No void layer was observed at ion implantation stage for sample with $5 \times 10^{15} \text{ cm}^{-2}$ -hydrogen atoms. Laser irradiation at $4.9 \times 10^4 \text{ W/cm}^2$ formed a void layer with a void ratio of 0.013 at a depth of 255 nm.

DOI:10.2961/jlmn.2012.01.0018

Keywords: SOI, hydrogen implantation, laser heating, void layer, optical reflectivity

1. Introduction

Hydrogen ion implantation is an attractive method for fabrication of the silicon-on-insulator structure [1]. Highly dense hydrogen atoms are easily incorporated in the silicon surface regions by ion implantation method. Subsequent heating causes evaporation of hydrogen and formation of a buried void layer in silicon, which results in removing the top silicon layer from the underlying silicon substrate. Narrow and flat void layer is suitable for making removing surface flat and smooth.

In this paper, we propose millisecond-rapid laser heating to form buried void layer in hydrogen implanted silicon substrates. High intensity laser irradiation can rapidly heat the silicon surface region to a high temperature [2]. Laser rapid heating will easily evaporate hydrogen atoms implanted in silicon. Many silicon bonds will be broken associated with the hydrogen evaporation so that small voids will be formed in the silicon surface region. Laser rapid heating will simultaneously cure lattice damages caused by hydrogen ion implantation. We report analysis of optical reflectivity spectra of samples implanted with hydrogen atoms and subsequently heated by laser irradiation. The analysis confirms buried void layer formation. It also determines the depth of void layer and the density of voids. Moreover, the analysis reports change in crystalline volume ratio in the silicon surface region with laser irradiation. Via those analyses, we discuss the condition of laser-induced formation of buried void layer.

2. Experimental Details

P-type silicon substrates with a resistivity of 20 Ωcm and a thickness of 520 μm were prepared. The both surfaces were coated with 100-nm-thick thermally grown SiO₂ layers. Hydrogen 2H⁺ ions were implanted to the top surface of silicon substrates at 60 keV, with doses of 5×10^{15} and $3 \times 10^{16} \text{ cm}^{-2}$. The in-depth profile of hydrogen atoms were estimated by numerical calculation program, as shown in Fig. 1. Hydrogen atoms had a peak concentration at 230 nm deep from the silicon surface.

Samples were irradiated with infrared semiconductor laser. Figure 2 shows a schematic apparatus of laser heating. A 940-nm infrared semiconductor laser beam with a maximum power of 23 W was introduced by an optical fiber.

The optical fiber and optics with lens were mounted on a X-Y mobile stage. The laser was moved in the Y-direction. It was also moved in the X-direction with a step of 100 μm. The laser beam was focused by lens to a spot with a Gauss-

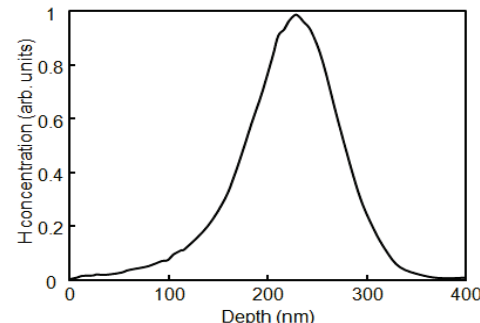


Fig. 1: In-depth concentration of hydrogen atoms calculated by TRIM.

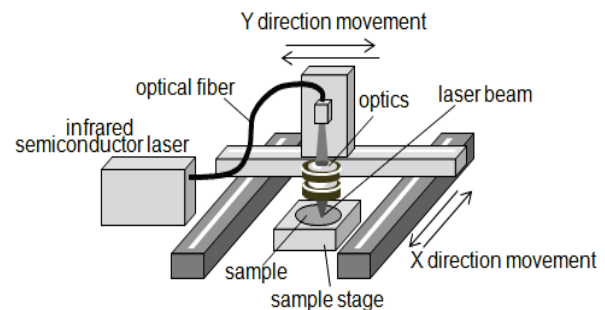


Fig. 2: Schematic apparatus of infrared semiconductor laser heating.

ian intensity distribution with a diameter of 200 μm at full width at half maximum at the sample surface. Samples were placed on a stage at a normal direction to the laser beam. The samples were irradiated with the laser beam at power densities ranging from 4.0×10^4 to $4.9 \times 10^4 \text{ W/cm}^2$ for 4 ms conducted by moving the laser beam at 5 cm/s. A numerical heat flow simulation estimated that the silicon surface was heated to 780°C at maximum by laser heating at $4.9 \times 10^4 \text{ W/cm}^2$ for 520 μm -thick samples.

Optical reflectivity spectra were measured between 250 and 1100 nm using a conventional spectrometer. They were analyzed using a numerical calculation program, which was constructed with the optical interference effect with multiple-layered structures with top silicon layer and underlying void layers, as shown in Fig. 3 [3,4]. The optical reflectivity depends on the complex refractive indexes of those layers. Using the effective-medium approximation model, we introduced the complex refractive indexes, n_α for the top silicon layer as partially amorphized layer with a crystalline volume ratio, α , and n_β for the void layer as partially void layers with a void ratio β , given as

$$n_\alpha = \alpha n_c + (1-\alpha) n_a \quad , \quad (1)$$

$$n_\beta = \beta n_{\text{air}} + (1-\beta) n_\alpha \quad , \quad (2)$$

where n_c , n_a , and n_{air} are complex refractive indexes of crystalline silicon, amorphous silicon, and air($=1$). The values of the parameters of thickness of each layer, α , and β were changed for each layer to calculate the reflectivity. Difference in reflectivity spectra was introduced by subtracting spectrum of samples from the spectra of single crystalline silicon to precisely analyze structure of surface regions.

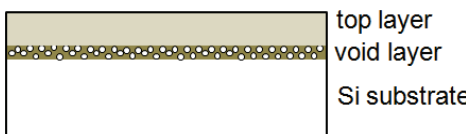


Fig. 3: Schematic structure of silicon surface region caused by hydrogen ion implantation and laser heating.

Figure 4 shows calculated optical reflectivity spectra of 255-nm-thick partially amorphized layer with α of 0.8 at the top surface, 10-nm-thick partially void layer with β of 0.2 underlying 255-nm-thick perfect crystal-line top layer, and single crystalline silicon (a), and differences in those optical reflectivity spectra, which were obtained by subtracting optical reflectivity spectra of the layered structures by the optical reflectivity spectrum of single crystalline silicon (b). The E_1 and E_2 peaks around 280 and 370 nm appeared for every case in Fig. 4(a). In the case of the partially amorphized top layer, those peak heights were slightly lower than that of single crystalline because those peaks sensitively reflect the density of states of crystalline silicon. The optical reflectivity spectra of calculated samples with

the partially amorphized top layer and partially void layer had small fringes from 400 to 1100 nm. Those fringes resulted from the optical interference effect caused by the different in complex refractive indexes between the top partially amorphized layer and crystalline silicon, or the top crystalline layer and buried void layer. The fringes appeared in the positive region in the difference spectra for sample with the partially amorphized top layer, as shown in Fig. 4(b) because amorphous silicon has higher refractive indexes than those of crystalline silicon between 400 and 1100 nm. On the other hand, the fringes oscillated almost symmetrically on the zero point in the case of the buried void layer, as shown in Fig. 4(b). The results of Fig. 4 indicate that analysis of optical reflectivity spectra in ultraviolet, visible, and infrared regions provide information on the void layer and crystalline volume ratio near surface regions. The most possible in-depth distributions of the void and crystalline volume ratio were obtained by fitting calculated spectra to experimental ones.

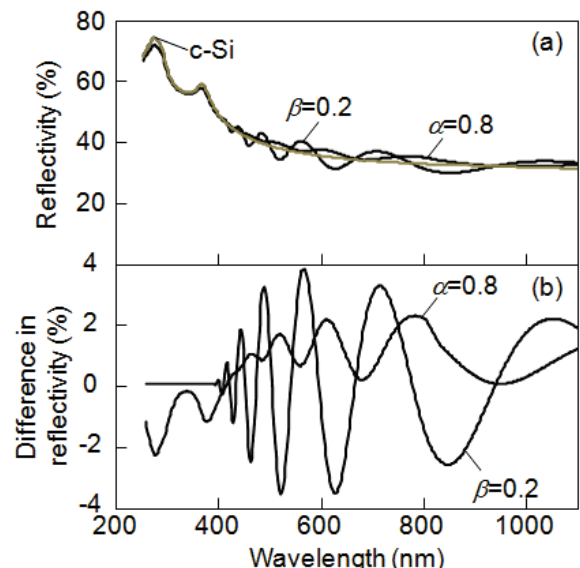


Fig. 4: Calculated optical reflectivity spectra (a) and differences in those reflectivity spectra (b) for the cases of 255-nm-thick partially amorphized top layer with α of 0.8, 10-nm-thick partially void layer with β of 0.2 at a depth of 255 nm as well as single crystalline silicon shown in (a).

3. Results and discussions

Solid curves in Fig. 5 show differences in experimental reflectivity spectra of samples as- $5 \times 10^{15} \text{ cm}^{-2}$ -hydrogen-ion implanted (a), laser annealed at $4.2 \times 10^4 \text{ W/cm}^2$ (b), and $4.9 \times 10^4 \text{ W/cm}^2$ (c). Dashed curves in Fig. 5 show calculated differences in reflectivity spectra conducted using our theory described above. The as-ion-implanted sample shows small fringes between 400 and 1100 nm. They appeared in the positive region, as shown in Fig. 5(a). It means that the surface region was partially amorphized by hydrogen ion implantation. Laser heating at $4.2 \times 10^4 \text{ W/cm}^2$ increased the amplitude of fringes and moved them

to zero level, as shown in Fig. 5(b). It means that a void layer was formed in silicon substrate by the laser heating. Laser heating at 4.9×10^4 W/cm² further increased the amplitude of fringes. The fringes oscillated almost symmetri-

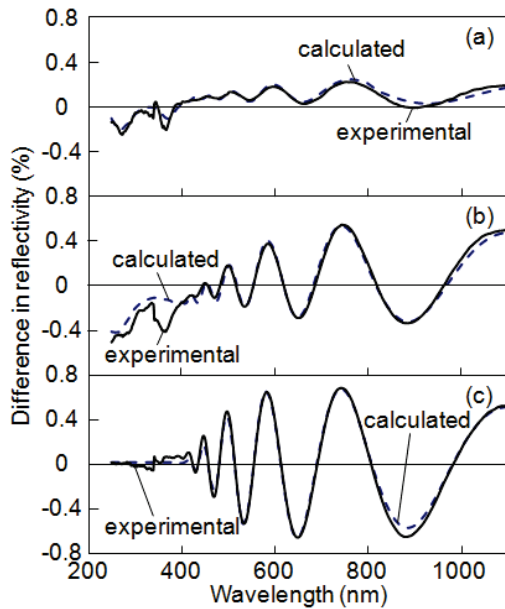


Fig. 5: Differences in experimental reflectivity spectra of samples as- 5×10^{15} -cm⁻²-hydrogen-ion implanted (a), laser annealed at 4.2×10^4 W/cm² (b), and 4.9×10^4 W/cm² (c). Dashed curves show calculated differences in reflectivity spectra.

cally on the zero point as shown in Fig. 5(c). On the other hand, the phase of oscillation of the fringes was the same between Fig. 5(b) and 5(c). Those mean that the top surface region maintained the same thickness, and that the void ratio β was increased by the laser heating at 4.9×10^4 W/cm².

Solid curves in Fig. 6 show differences in experimental reflectivity spectra of samples as- 3×10^{16} -cm⁻²-hydrogen-ion implanted (a), laser annealed at 4.0×10^4 W/cm² (b), and 4.2×10^4 W/cm² (c). Dashed curves in Fig. 6 show calculated differences in reflectivity spectra. The as-ion-implanted sample shows fringes between 400 and 1100 nm with rather large amplitudes compared with the samples implanted with 5×10^{15} -cm⁻²-hydrogen ions, as shown in Figs. 6(a) and 5(a). The oscillation central point was close to the zero point, as shown in Fig. 6(a). It means that 3×10^{16} -cm⁻²-hydrogen-ion implantation formed buried void layer and partially amorphized the top surface region simultaneously. Some hydrogen atoms probably recombined and made hydrogen molecules to increase gas pressure in silicon during their implantation. Hydrogen gases broke silicon bonds. Laser heating at 4.2×10^4 W/cm² increased the amplitude of fringes, as shown in Fig. 6(c). It means that the void ratio β was increased by laser heating. The phase of oscillation of the fringes was almost the same among Figs. 6(a) to 6(c). It indicates that the void layer maintained the same depth during implantation and laser heating.

Best fitting calculated spectra to the experimental spectra shown in Figs. 5 and 6 gave information of sample structures. Figure 7 shows summary of analysis of α (a), the thickness at the top layer (b), the thickness of the void layer (c), and β (d) as functions of the laser intensity. In-

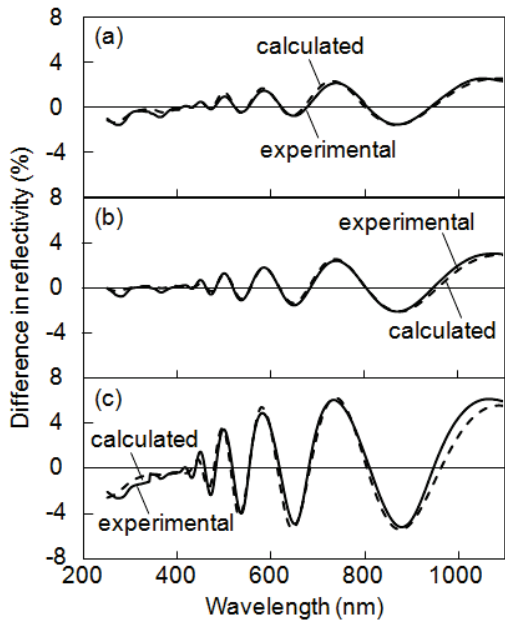


Fig. 6: Differences in experimental reflectivity spectra of samples as- 3×10^{16} -cm⁻²-hydrogen-ion implanted (a), laser annealed at 4.0×10^4 W/cm² (b), and 4.2×10^4 W/cm² (c). Dashed curves show calculated differences in reflectivity spectra.

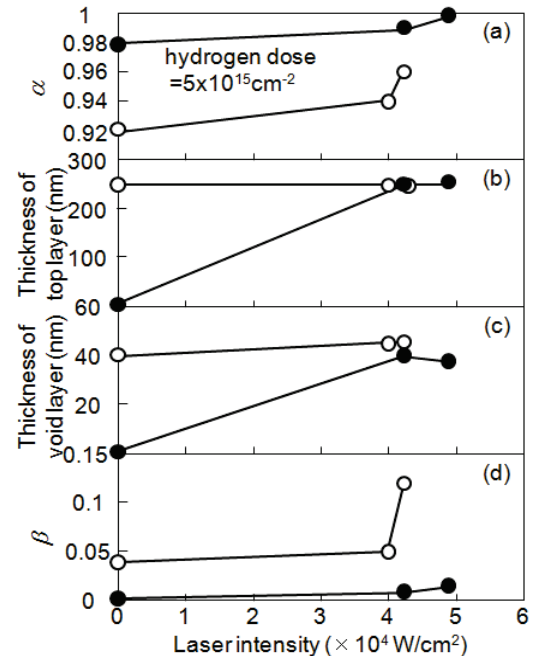


Fig. 7: α (a), thickness at the top layer (b), thickness of the void layer (c), and β (d) as functions of the laser intensity for samples implanted with hydrogen at 5×10^{15} (solid marks) and 3×10^{16} cm⁻² (open marks).

crease in α shown in Fig. 7(a) means that the top silicon layer was recrystallized well by laser rapid heating. The void layers were formed 255 and 250 nm from the surface for samples implanted with 5×10^{15} and $3 \times 10^{16} \text{ cm}^{-2}$ hydrogen atoms respectively, as shown in Fig. 7(b). The depths were just close to the peak concentration of hydrogen atoms implanted at 60 keV, as shown in Fig. 1. The void layers had a thickness of about 40 nm, as shown in Fig. 7(c). Small voids probably distributed in the regions. β was increased to 0.12 by laser heating at $4.2 \times 10^4 \text{ W/cm}^2$ for samples implanted with $3 \times 10^{16} \text{ cm}^{-2}$ -hydrogen atoms, although a void layer with β of 0.04 was already formed at implantation, as shown in Fig. 7(d). β was very low of 0.013 in the case of high power laser heating at $4.9 \times 10^4 \text{ W/cm}^2$ for samples implanted with $5 \times 10^{15} \text{ cm}^{-2}$ -hydrogen atoms. The low hydrogen concentration was not effective to form void layer. The sample maintained a smooth surface during all of process steps. Further optimization will achieve narrow and flat void layer with high void ratio.

4. Summary

We reported buried void layer formation by laser rapid heating of hydrogen implanted silicon substrates. P-type silicon substrates coated with 100 nm thick thermally grown SiO_2 layers were implanted with hydrogen atoms at 5×10^{15} and $3 \times 10^{16} \text{ cm}^{-2}$ at 60 keV. An apparatus of 940-nm infrared semiconductor laser irradiation was constructed with an optics focusing the laser beam and a mechanical stage moving laser beam. Structural investigation was conducted by analysis of optical reflectivity spectra with a nu-

merical calculation program constructed with the optical interference effect with multiple-layered structures. $3 \times 10^{16} \text{ cm}^{-2}$ -hydrogen implantation caused a void layer with a void ratio of 0.04 at a depth of 250 nm close to the position of hydrogen peak concentration. Laser irradiation at $4.2 \times 10^4 \text{ W/cm}^2$ increased the void ratio to 0.12. On the other hand, no void layer was observed at ion implantation stage for sample with $5 \times 10^{15} \text{ cm}^{-2}$ -hydrogen atoms. Laser irradiation at $4.9 \times 10^4 \text{ W/cm}^2$ formed a void layer with a void ratio of 0.013 at a depth of 255 nm..

Acknowledgments

This work was partly supported by Grant-in-Aid for Science Research C (No. 22560292) from the Ministry of Education, Culture, Sports, Science and Technology of Japan, and Takahashi Industrial and Economic Research Foundation.

References

- [1] S. Personnic, A. Tauzin, K. Bourdelle, F. Letertre, N. Kerneves, F. Laugier, N. Cherkashin, A. Claverie and R. Fortunier, IIT2006 AIP conference proceedings (2006) pp.65-68
- [2] K. Ukawa, Y. Kanda, T. Sameshima, N. Sano, M. Naito and N. Hamamoto: Jpn. J.Appl. Phys. 49 (2010) 076503.
- [3] M. Born and E. Wolf: Principles of Optics (Pergamon, New York,1974) Chaps. 1 and 13.
- [4] T. Sameshima, Y. Matsuda, Y. Andoh, and N. Sano, Jpn. J.Appl. Phys. 47 (2008) 1871.

(Received: June 3, 2011, Accepted: January 16, 2012)